JOURNAL OF CATALYSIS **176,** 192–203 (1998)
ARTICLE NO. CA982023

# Elementary Mechanistic Steps and the Influence of Process Variables in Isobutane Alkylation over H-BEA

Gautam S. Nivarthy, Yingjie He, K. Seshan, and Johannes A. Lercher[1]

*Faculty of Chemical Technology, University of Twente, Postbus 217, Enschede 7500AE, The Netherlands*

Received October 3, 1997; revised December 23, 1997; accepted December 23, 1997

**Liquid phase conversion of n-butene in excess iso-butane was investigated over zeolite BEA as catalyst in a continuously operated slurry reactor. Single and multiple alkylation and cracking were the main reaction pathways. Only saturated products were observed indicating that hydride transfer reactions were fast, compared to desorption of olefins under the experimental conditions chosen. An optimal reaction temperature of 350 K was identified for single alkylation, higher reaction temperatures favoring cracking of intermediately formed products and lower temperatures, multiple alkylation. Under optimum reaction conditions over 80 wt% butene was converted via single alkylation. The $C_8$ product selectivity is determined by the balance between isomerization of the $C_8$ alkoxy and the hydride transfer to release iso-octanes from the acid sites. Once desorbed from an acid site, the alkanes do not isomerize. Independent of the space velocities the catalyst and, hence, the individual acid sites deactivate after approximately 30 butene turnovers at 350 K by deposition of polyalkylates. A simplified reaction model for alkylation over solid acid catalysts and the implications for catalyst design are discussed.** 

## INTRODUCTION

Acid catalysed alkylation of isobutane with butene draws increasing industrial interest due to the rising demand for high octane gasoline and the environmental concerns associated with the existing processes for isobutane alkylation (1). The present commercial routes for alkylation rely on the use of $H_2SO_4$ and HF as acid catalysts (2). The toxicity and the environmental concerns linked with these liquid acid catalysts are well known (3). Consequently, the use of alternative such as solid acid catalysts are currently being explored.

Zeolites with high acid site concentrations have been suggested as potential catalytic materials for isobutane/butene alkylation (3). Studies have focussed on large pore materials such as BEA (4), Y (5), USHY (6), MCM-22 (7), MCM-36, and MCM-49 (8, 9) as smaller pore zeolites preclude the formation of bulky $C_8$ alkanes such as trimethylpentanes (TMPs). However, until recently (3, 5, 10–13), most literature indicated a very rapid deactivation of zeolite catalysts. Especially, when the reaction was carried out in a fixed bed reactor, butene oligomerisation dominated and the catalysts deactivated within a few minutes time on-stream. Comparing catalysts or even drawing mechanistic conclusions under these rapidly deactivating conditions is difficult.

Zeolite BEA has been studied extensively under fixed bed conditions as a catalyst for isobutane/2-butene alkylation. Corma *et al.* (10) concluded that the strongest acid sites of this zeolite were responsible for the production of the desirable alkylate molecules, particularly the trimethylpentanes (TMPs) and that dealumination of the zeolite and the presence of extraframework aluminium oxide species in the vicinity of the catalytic sites was detrimental for activity and selectivity towards alkylation (13). However, compared to other large pore zeolites containing 12-member ring pores such as FAU, MOR, or MCM-22, BEA showed better catalyst stability and higher alkylate selectivity. More recently, de Jong and co-workers (14, 15) reported that low olefin space velocities in a well stirred slurry reactor allowed to achieve high catalyst lifetimes with BEA and USHY. It was elegantly shown there that the use of fundamental chemical engineering principles dramatically improved the catalyst performance.

Under these conditions it is now possible to explore reliably the factors influencing catalyst lifetime and product yields to further develop the simplified reaction models of solid acid catalyzed alkylation proposed, e.g. in Refs. (13, 14). Here, the role of the reaction conditions, the elementary steps of the reaction and the nature of the acid sites catalyzing the reaction are central.

## EXPERIMENTAL

### *Catalyst*

Zeolite BEA was obtained from PQ Corporation *(806 B-25 LOT #B-12)* in the *as-synthesized* form. The zeolite was converted to its acidic form by initially calcining the

[1] Corresponding author. E-mail: j.a.lercher@ct.utwente.nl



0021-9517/98 $25.00

sample with dried $N_2$ (50 ml/min) using a temperature program consisting of heating at 1 K/min to 373 K, at 0.4 K/min to 413 K, at 2 K/min to 793 K and maintaining it at that temperature for 2 h and subsequently lowering the temperature to 573 K. At this temperature, a stream of dried air was passed over the catalyst instead of $N_2$ and the catalyst was once again heated at 2 K/min to 793 K, where a dwell time of 5 h was employed before finally cooling down the calcined material. Ion exchange was performed with 1 *M* $NH_4NO_3$ (Merck Co., 101188.1000) at neutral pH conditions at a temperature of 323 K, using approximately 7 ml liquid per gram solid. The procedure was repeated three times to ensure complete ion exchange. Finally, the sample was washed with distilled water. To eliminate $NH_3$, the sample was heated in a $N_2$ stream at 2 K/min to 773 K, where a dwell time of 2 h was employed.

*Physicochemical Characterization*

The $NH_3$ sorption/desoption measurements to determine acid site concentration were performed on a modified SETARAM TG-DSC 111 apparatus. For details of the measurements see Ref. (16). Temperature programmed desorption (TPD) curves were obtained on an independent setup equipped with a BALZERS QMS420 mass spectrometer to detect the concentration of desorbed substances (see Refs. (17, 18)).

EDAX spectroscopy to determine bulk Si/Al ratios was performed on a S800 Scanning Electron Microscope from Hitachi Co. equipped with a Kevex Quantum detector Energy Dispersive X-ray system allowing elemental compositions to be determined within an accuracy of 5% (relative). The instrument had a resolution at 5.9 keV of 109 eV. In order to ensure that the data collected was representative of the whole sample, scans were made at more than one location. The reproducibility verified indicates homogeneous zeolite particles. Calibration with a standard sample of ZSM-5 of known Si/Al ratio was performed prior to the measurements.

$Al^{27}$ MAS-NMR of H-BEA was performed on a multinuclear NMR spectrometer (Varian, Unity WB 400) equipped with a RT CP/MAS probe. The chemical shift was calibrated by using a sample of $Al(NO_3)_3 \cdot 9H_2O$. The spectra were obtained at 8 kHz spinning speed with an excitation of pulse of 0.6 $\mu$s to quantify data (19).

FTIR spectra of catalyst samples were collected on a Bruker IFS 88 spectrometer with a spectral resolution of 4 $cm^{-1}$ using a home built vacuum cell allowing all sample manipulation to be performed *in situ* in the transmission-absorption mode.

*Catalytic Reactions*

The reactions were carried out in a continuously operated, well-stirred, 50-ml Hastelloy C-276 microclave (Autoclave Engineers Co.) system shown schematically in Fig. 1. The reactor could be operated between 273 and 613 K at pressures ranging upto 350 bar. In a typical run, the reaction temperature was lower than 373 K and the pressure between 20 and 50 bar. Feed tanks A and B were filled, respectively, with isobutane and a mixture of isobutane with cis-2-butene (Indugas). An automated 4-port valve was used to switch between the two flows. The reactants were fed to the reactor as liquids using $N_2$ head pressure and using liquid mass flow controllers. Stirring speeds of 3500 rpm were employed using a pitched blade turbine impeller.

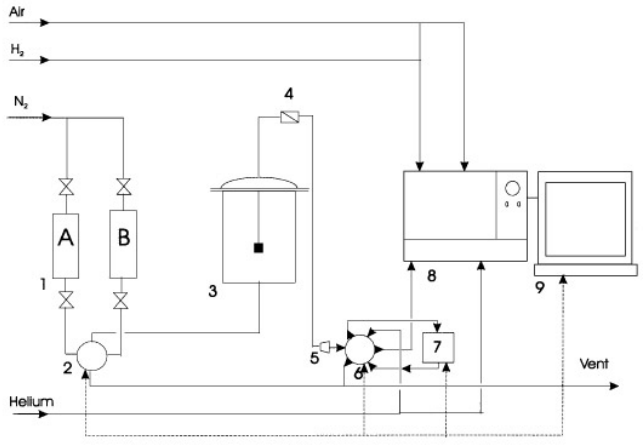


**FIG. 1.** Simplified schematic of the setup used for studying solid acid catalysed isobutane alkylation in the slurry phase (1, feed tanks; 2, 4-port switching valve; 3, autoclave with pitched blade turbine impeller; 4, filter; 5, back pressure regulator; 6, 6-port valve; 7, multiposition valve with sample loops; 8, gas chromatograph; 9, computer interface).

Reactants and products were analysed with a gas chromatograph (Hewlett Packard, 5890) equipped with a FID detector and a 35-m long DB-1 column (J&W Scientific) with helium as the carrier gas. The peaks were assigned using standard alkylate and naphtha samples from Supelco Co. Separation of 2,5-dimethylhexane from 2,2,3-trimethylpentane was not achieved.

A typical reaction procedure consisted of first filling up the reactor containing the catalyst (preactivated *ex-situ* for 2 h at 473 K in air and *in situ* at 473 K for 2 h) completely with isobutane and subsequently introducing a mixture of isobutane and cis-2-butene with a predefined P/O ratio. Olefin space velocities of 0.05–0.4 $h^{-1}$ were obtained by controlling the flow rate of liquid.

Samples of deactivated catalyst were analyzed *ex situ* for their carbon and hydrogen content using an elemental analyser (Fisons Instruments, EA 1108) which works on the principle of flash dynamic combustion at 2000 K, followed by the analysis of the off gases using a gas chromatograph equipped with a thermal conductivity detector (TCD).

## RESULTS

### *Catalyst Characterisation*

The zeolite BEA used in this work is a well-crystallized material with a primary particle size of 0.5 $\mu$m as to be seen from the SEM picture in Fig. 2. The Si/Al ratio of the sample determined by EDAX was 11 for the uncalcined sample and 15 for the H-BEA sample indicating moderate leaching of framework Al species during the ion exchange and catalyst pretreatment procedures. The $^{27}$Al MAS-NMR spectrum of the calcined sample shown in Fig. 3 indicates the presence of substantial concentrations of extra lattice alumina. The ratio of the peaks corresponding to tetrahedral and octahedrally coordinated Al was 1.6.

To quantify the concentration of Lewis acid sites in the material, pyridine was adsorbed at 300 K with an equilibrium pressure of $10^{-2}$ mbar. Subsequently, the cell was evacuated at $10^{-6}$ mbar to eliminate physisorbed pyridine. The IR spectrum after this treatment is shown in Fig. 4. The bands at 1545 and 1454 cm$^{-1}$ represent pyridine sorbed on Brønsted and Lewis acid sites, respectively. The ratio of the concentration of these sites (Brønsted/Lewis) using the extinction coefficients of Ref. (20) was 1.6. Note that this value agrees excellently with the ratio of extraframework

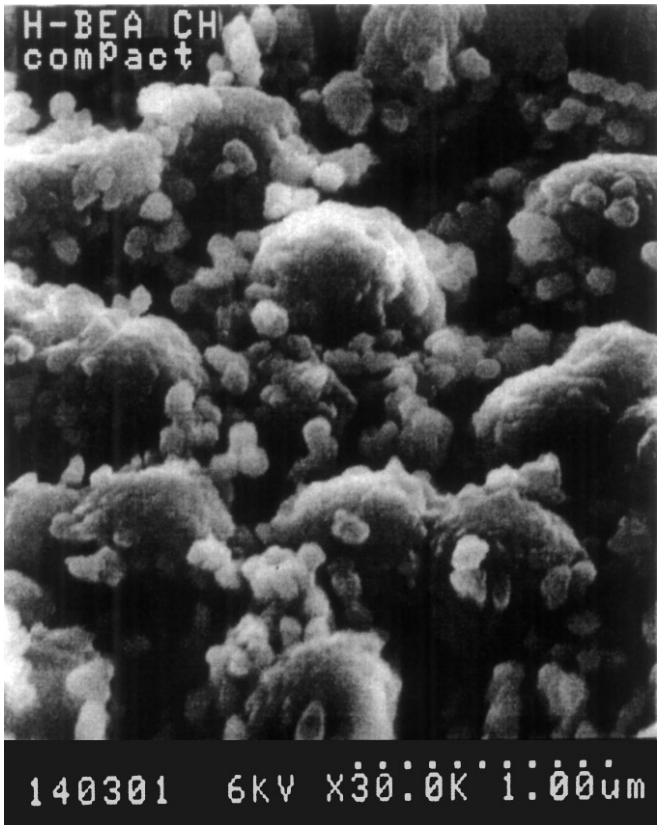


**FIG. 2.** SEM picture of H-BEA. Besides the 0.5 $\mu$m agglomerates, smaller particles less that 0.1 $\mu$m are visible.

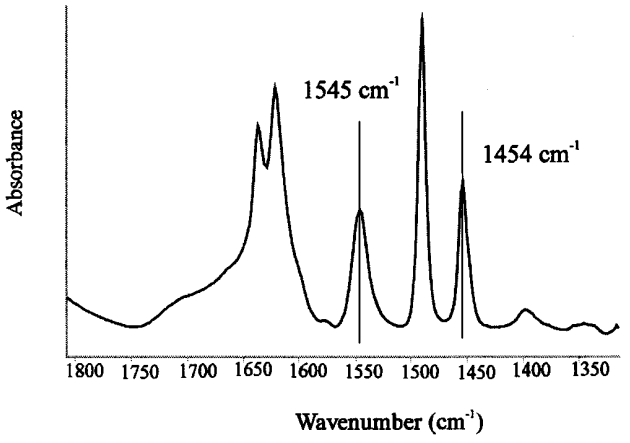


**FIG. 3.** FT-IR spectrum of pyridine chemisorbed on the acidic sites of H-BEA at 323 K. Complete coverage of sites was ensured. The peaks at 1545 and 1454 cm$^{-1}$ respectively correspond to Brønsted and Lewis bonded pyridine and the ratio of the amount of Brønsted to Lewis sites is determined to be 1.6.

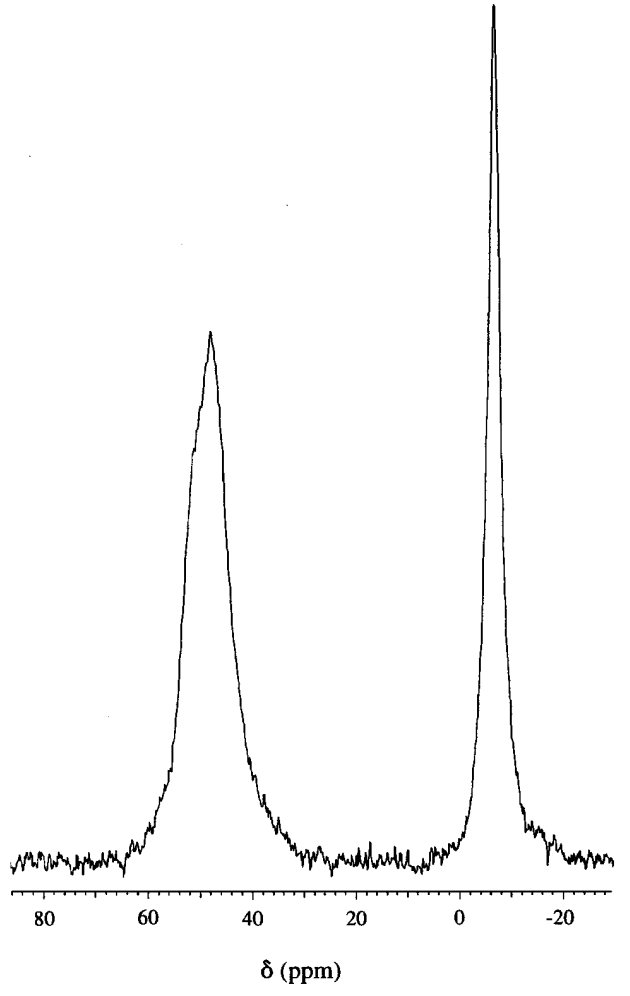


**FIG. 4.** $^{27}$Al MAS-NMR spectra of H-BEA catalyst. The two peaks were integrated to obtain the concentration of tetrahedral and octahedral Al sites.

to framework aluminum as determined by NMR. Quantification of the acid site concentration via temperature programmed desorption (t.p.d.) of pyridine yielded a slightly higher value, i.e., Brønsted and Lewis site concentrations of 0.4 and 0.2 mmol/g, respectively.

The concentration of acid sites retaining $NH_3$ at 373 K was determined by sorption/desorption experiments. A weighed sample of zeolite was saturated with 2 mbar ammonia at 373 K, followed by evacuation for 7 h. The ammonia retained was used to estimate the concentration of acid sites on the sample by assuming a stoichiometry of one adsorbed ammonia per acid sites (see e.g., Ref. (16)). By temperature-programmed desorption of the chemisorbed ammonia the gravimetric results were confirmed. The concentration of acid sites determined so was 0.7 mmol/g being approximately 70% of the maximum concentration of sites calculated from the chemical composition of BEA using the Si/Al ratio determined by EDAX. The BET surface area and the micropore volume of the H-BEA sample were determined to be 514 $m^2/g$ and 0.108 cc/g, respectively, using $N_2$ sorption.

*Kinetic Experiments*

*Influence of temperature and pressure on alkylation.* Alkylation of iso-butane with n-butene was carried out at four different temperatures between 323 and 423 K. The highest temperature corresponds to operation under supercritical conditions with respect to isobutane. The reaction pressure was increased in parallel with temperature (from 25 bar at 323 K to 50 bar at 423 K) in order to ensure only a condensed phase in the reactor. In all experiments, the initial n-butene conversion was 100% and once steady state was achieved the product composition hardly varied until the catalyst began to markedly deactivate. The average product selectivities, obtained under conditions of complete butene conversion are plotted in Fig. 5 as a function of temperature. It is seen that at lower temperatures, the $C_{9-12}$ products dominate, while at higher temperatures, the fraction of $C_{5-7}$ products increases. The production of the desirable $C_8$ products reaches an optimum around 350 K.

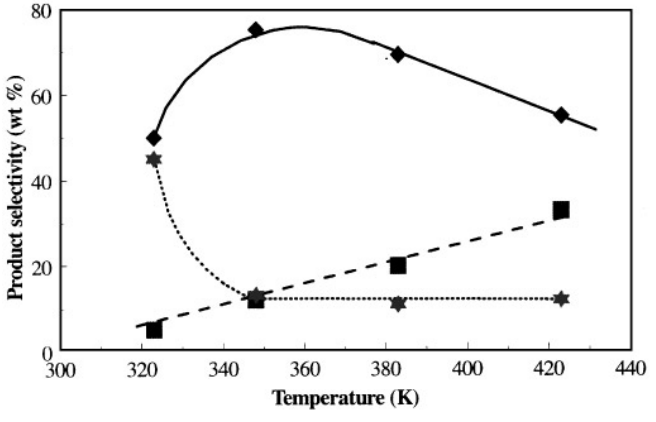


**FIG. 5.** Variation of alkylation selectivity (time averaged under stable butene conversion conditions) to various fractions with temperature (◆, $C_8$; ★, $C_{9-12}$; and ■, $C_{5-7}$). Pressures of 20, 30, 40, and 50 bar were used in the four cases in order to maintain a condensed phase.

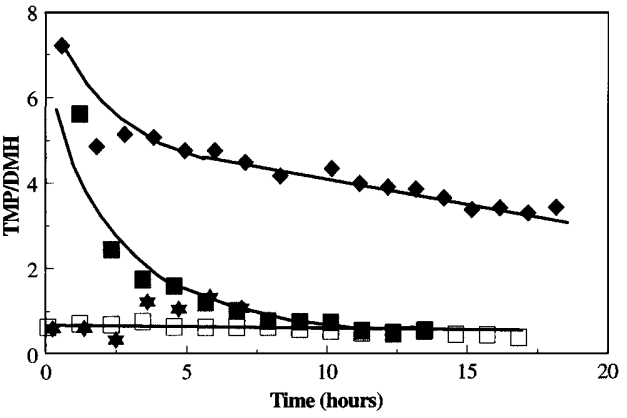


**FIG. 6.** Variation of TMP/DMH ratio with time on stream at different temperatures (◆, 348 K; ■, 323 K; ★, 383 K; □, 423 K) (butene conversion was 100% in all cases).

The alkylation products consisted of trimethylpentanes (TMP) and dimethylhexanes (DMH). The TMP/DMH ratio is plotted in Fig. 6 as a function of time on stream. The highest TMP/DMH ratio was obtained at 348 K when the $C_8$ fraction also dominated. At higher temperatures, however, the TMP/DMH ratio approaches 0.1 being closer to the thermodynamic equilibrium value. At 323 and 348 K, relatively high TMP/DMH ratios were obtained at initial times on stream which decreased with time on stream.

When the total pressure was varied between 20 and 50 bar at 348 K with an olefin space velocity of 0.2 $h^{-1}$, changes in the product selectivity or catalyst lifetime of zeolite H-BEA were not observed. It should be emphasized at this point that operation under supercritical conditions on H-BEA apparently did not markedly influence the product selectivity other than expected, due to the increase in temperature. As the reaction temperature of 348 K and 25 bar total pressure were found to be optimal, these conditions were employed in all further experiments.

*Activity and selectivity.* According to the simplified kinetic model of Mesters *et al.* (14), the most important factors influencing the activity and the lifetime of the catalyst are the paraffin/olefin (P/O) ratio, the olefin space velocity (OSV) and the catalyst loading. The kinetic model indicates that the catalyst rapidly deactivates, once butene conversions decrease below 100%. We chose our process conditions, therefore, such that 100% butene conversion was seen for a substantial length of time. At a space velocity of 0.2 $h^{-1}$ with a P/O ratio of 17, we observed stable catalyst performance for 15 h as demonstrated in Fig. 7. The distribution of the various fractions of the product stream obtained under these conditions are compiled in Fig. 8. Initially, a high fraction of doubly alkylated molecules appeared

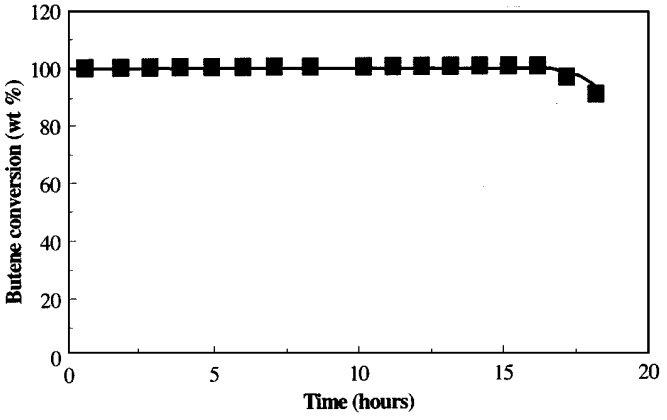


FIG. 7. Butene conversion during isobutane alkylation with cis-2-butene on H-BEA at 348 K (p = 25 bar, OSV = 0.2 $h^{-1}$, P/O = 17).

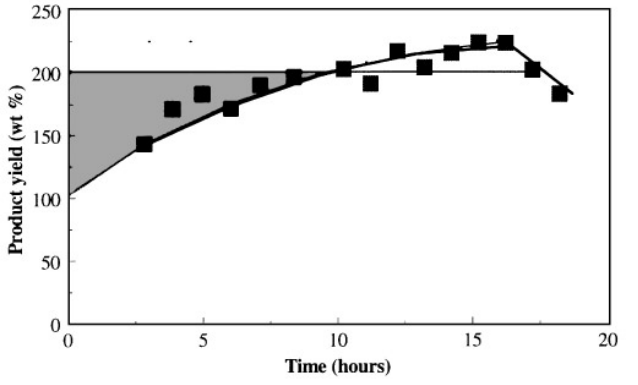


FIG. 9. Yield profile during isobutane/butene alkylation (T = 348 K, p = 25 bar, OSV = 0.2 $h^{-1}$, P/O = 17). All $C_5^+$ molecules are accounted in the yield. The shaded region is the butene that is not accounted for in the product stream and hence must manifest as (hydro)carbon deposit.

which decreased to the steady state value of 10 wt% within the first 7 h. In parallel, the octanes increase from 30 to 80 wt%. Smaller (cracked) products approach 10 wt% after 7 h. Once deactivation started, the yield of doubly alkylated products increased at the expense of the octanes. The yield of cracked products was not influenced. The alkylate yield, calculated as the weight of alkylate per unit weight of butene fed to the reactor, increased gradually (see Fig. 9) to about 220 wt%. The alkylate yield at a particular time was determined by dividing the weight of the alkylate products by the weight of the butene charged to the reactor at that time. Note that theoretically, 204 wt% are expected from the reaction of isobutane with butene to produce isooctane. The grey area in Fig. 9 corresponds to the fraction of butene molecules fed to the reactor (irreversibly) deposited on the catalyst, expressed as a weight percent. Dividing this area by the area below the curve, we obtain the butene selectivity to deposit formation estimated to be approximately 13 wt%. The area above 204 wt% under the yield curve is attributed to the release of polyalkylate species from the catalyst surface as the reaction proceeds.

Within the octane product fraction (Fig. 10) trimethylpentanes (TMPs) dominated, 2,2,4-trimethylpentane being

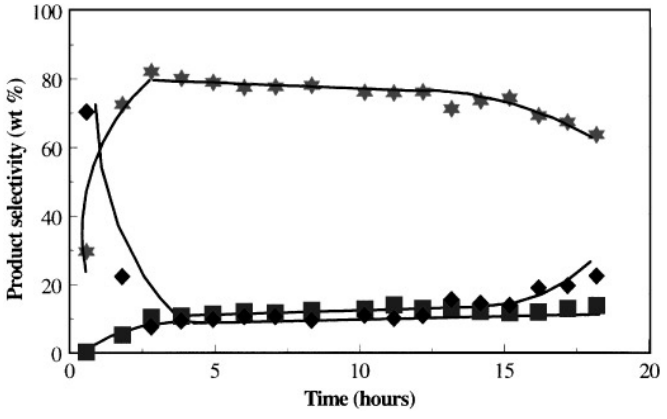


FIG. 8. Product selectivity during isobutane/cis-2-butene alkylation on H-BEA as a function of time on stream (T = 348 K, p = 25 bar, OSV = 0.2 $h^{-1}$, P/O = 17; ★, $C_8$; ◆, $C_{9-12}$; ■, $C_{5-7}$).

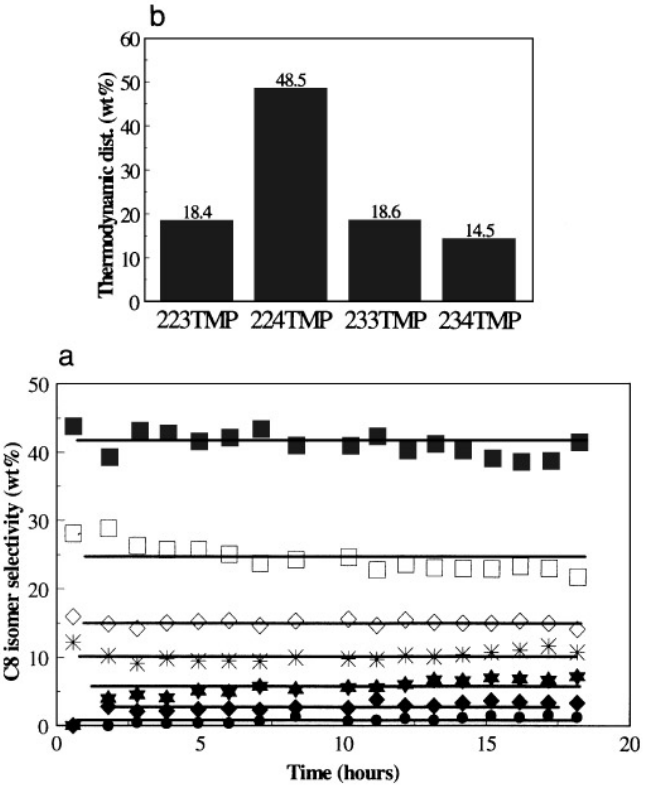


FIG. 10. (a) The distribution of TMP and DMH isomers during isobutane/cis-2-butene alkylation. (T = 348 K, p = 25 bar, OSV = 0.2 $h^{-1}$, P/O = 17) (■, 224 TMP; □, 234 TMP; ◇, 233 TMP; *, 23 DMH; ★, 25 DMH/223 TMP; ◆, 24 DMH; ●, 34 DMH). (b) The thermodynamic distribution of the TMP isomers at 348 K. Note that under the same conditions, DMH isomers are much more stable as discussed in text.

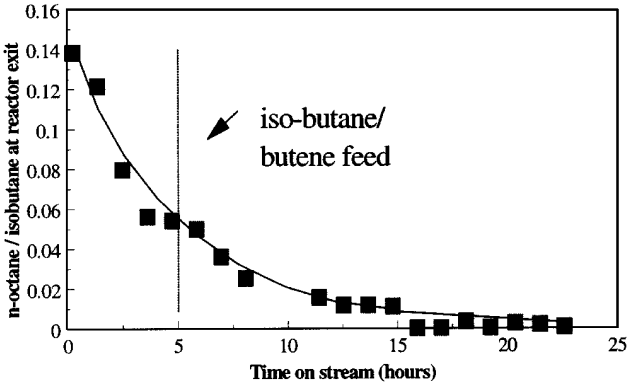


FIG. 11. n-octane elution from presaturated H-BEA catalyst in the alkylation reactor (T = 348 K, p = 25 bar).

the most abundant. This was followed by 2,3,4-trimethylpentane and 2,3,3-trimethylpentane. Dimethylhexanes which are thermodynamically more favored than trimethylpentanes were obtained in lower quantities than TMPs.

As all branched products are quite bulky the question arises in how far secondary isomerization (of retained octanes) contributes to the product patterns observed. In order to explore this, the catalyst was first presaturated with n-octane and iso-butane was passed over subsequently with a flow rate of 8.5 g/h at 348 K. n-Octane isomerisation was not observed as indicated the steady elution of n-octane in Fig. 11. Upon switching the feed to an isobutane–butene mixture, paraffin alkylation was observed, again without inducing changes in the $C_8$ isomer selectivity compared to the run performed in the absence of n-octane. The elution of n-octane continued uninterrupted. Thus, we conclude that n-octane does not react under the conditions reported here.

To explore the role of butene isomerisation for the product selectivities, alkylation was also performed with 1-butene as alkylating agent. Figure 12 demonstrates that the $C_8$ selectivity obtained with 1-butene as the alkylating agent was identical to that obtained with cis-2-butene.

In order to study the reaction over a longer time span, lower olefin space velocities (0.02 and 0.05 $h^{-1}$) realized by using higher catalyst loadings, higher P/O feed ratios or lower flow rates of the feed mixture into the reactor, were employed. The reaction conditions used and the $C_8$ paraffin selectivity as a function of time are compiled in Fig. 13. It can be seen that with time on-stream the selectivity to 2,2,4-TMP increased at the expense of the selectivity to other TMPs, particularly 2,3,4-TMP. The TMP/DMH ratio (5.5) was not influenced.

*Catalyst stability and deactivation.* In order to investigate the absolute turnover numbers that could be reached under various experimental conditions, the catalyst loading was varied at constant feed flow rate, resulting in a corresponding change in the olefin WHSV. At higher space velocities, lower catalyst lifetimes were observed (see Fig. 14). The total amount of butene converted before deactivation set in was calculated for each run by integrating the area below the conversion curves. A linear correlation between the total moles of butene converted and the moles of acid sites available was observed (see Fig. 15a). The butene turnover number before catalyst deactivation corresponds to the slope of this straight line and was found to be 40. Note that this indicates a surprisingly constant average number of turnovers on an individual site, before it becomes blocked by a larger alkoxy group or an alkane too large to desorb.

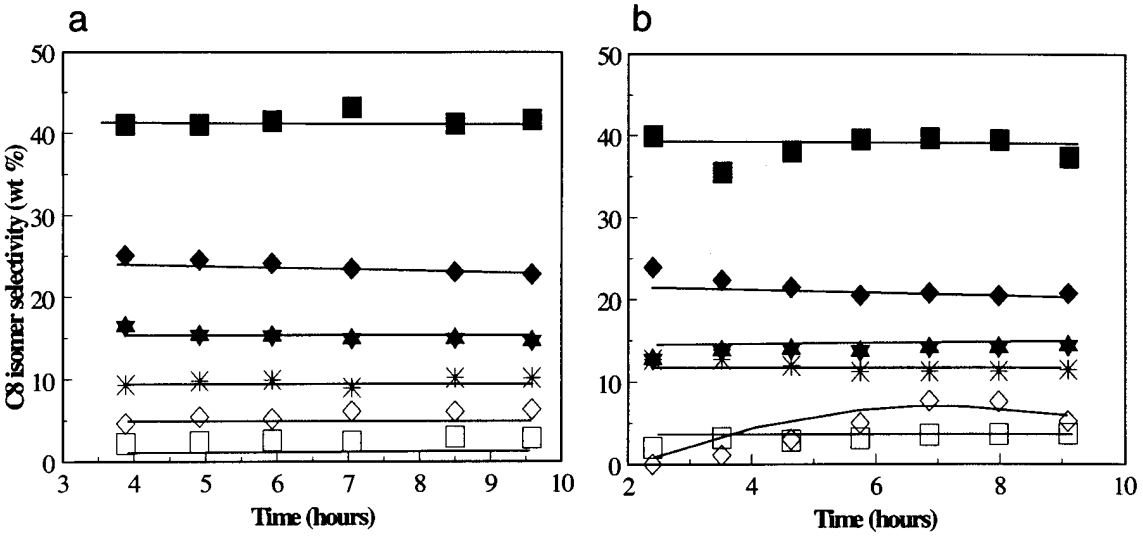


FIG. 12. $C_8$ isomer distribution is nearly identical in the case of isobutane alkylation with (a) cis-2-butene and (b) 1-butene (T = 348 K, p = 25 bar, OSV = 0.2 $h^{-1}$, P/O = 10) (■, 224 TMP; ◆, 234 TMP; ★, 233 TMP; □, 25 DMH/223 TMP; ◇, 24 DMH; *, 23 DMH).

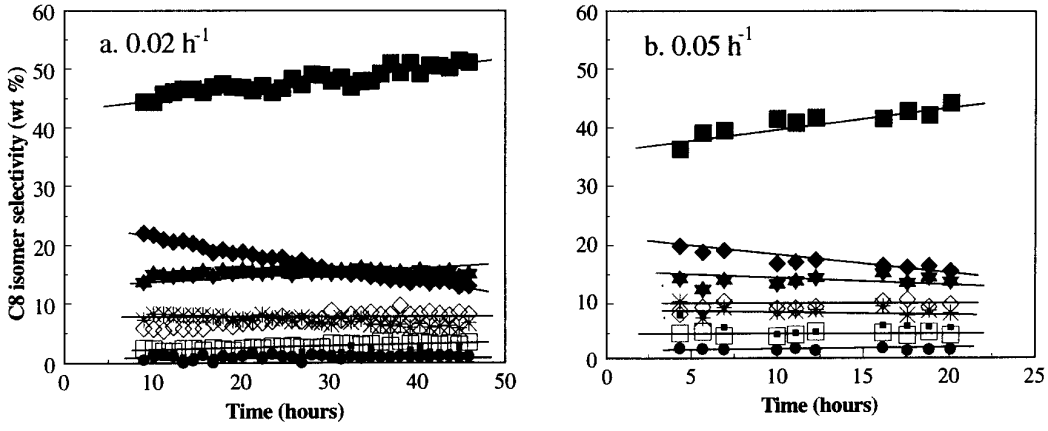


**FIG. 13.** Isomer selectivity during alkylation at very low space velocities (T = 348 K, p = 25 bar). (a) 0.02 $h^{-1}$ (catalyst weight = 2.8 g, P/O = 57); (b) 0.05 $h^{-1}$ (catalyst weight = 3.1 g, P/O = 27) (■, 224 TMP; ◆, 234 TMP; ★, 233 TMP; □, 24 DMH; ◇, 223 TMP/25 DMH; ∗, 23 DMH; ●, 34 DMH; ■, others).

Not all of these 40 butene molecules turned over per site contribute to the 204 wt% yield of alkylate observed. Two butene molecules are required for the initiation of the chain sequence by dimerization as discussed in the mechanistc scheme of Fig. 18. Approximately 10% of butene will alkylate an octylcarbenium ion and produce $C_{9-12}$ paraffins. Another 10% of butene is released at a later stage and contributes to yields above 204 wt% as seen in Fig. 9. Note that both effects have to be accounted for when estimating the fraction of butene irreversibly reacting in the pores of zeolite BEA.

The (hydro)carbon deposits on the deactivated catalysts at the end of the experiments were analyzed after each experimental run. Figure 15b shows the moles of carbon of these deposits achieved after establishing a level of 20% conversion of n-butene against the moles of carbon in butene converted. Again, a linear correlation was observed indicating a constant selectivity to form these deposits of approximately 14 wt% for H-BEA. Note that this is significantly larger than the value of 10.5% that had been estimated from the product selectivities in experiments where the catalyst was hardly deactivated (see the yield curve of Fig. 9). This indicates that on an already deactivated catalysts, i.e., one that begins to not fully convert butene, (hydro)carbon deposition accelerates.

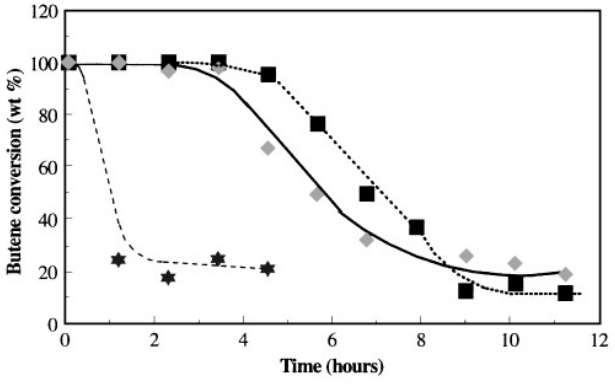


**FIG. 14.** Variation of catalyst lifetime with catalyst loading (T = 348 K, p = 25 bar) (■, WHSV = 0.2 $h^{-1}$; ◆, WHSV = 0.4 $h^{-1}$; ★, WHSV = 0.6 $h^{-1}$).

*Nature of the (hydro)carbon deposit on the catalyst.* In order to characterize the nature of the (hydro)carbon deposits a series of IR spectra were obtained using BEA catalyst. In separate experiments performed in the gas phase, an activated BEA catalyst was exposed first to cis-2-butene at a pressure of $10^{-3}$ mbar, then to isobutane at 1 mbar and finally, a sample saturated with isobutane at 1 mbar was exposed to $10^{-3}$ mbar of cis-2-butene. All the measurements were performed at 348 K. The spectra resulting from these individual sorption experiments are compiled in Figs. 16b–d, together with the IR spectrum of the activated BEA sample (Fig. 16a). The adsorption of isobutane results in a minor perturbation of the bridging hydroxyl group of zeolite BEA. However, upon adsorbing butene on the isobutane saturated zeolite or upon adsorbing butene alone, intense bands appear at 2960 and 2932 $cm^{-1}$ corresponding to $-CH_2$ and $-CH_3$ groups of the oligomeric species resulting from the olefin polymerization in the zeolite pores. A comparison of Figs. 16c and d indicates that in the presence of isobutane, butene polymerization is suppressed.

Additionally, the IR spectrum of a deactivated catalyst from a typical alkylation experiment was recorded for comparison (see Fig. 17). The bands observed at 2960, 2932, and 2880 $cm^{-1}$ indicate a high ratio of $-CH_2$ to $-CH_3$ groups on the deactivated catalyst and are characteristic of highly branched multiple alkylate species formed during the alkylation reaction. These bands differ in the ratio of their intensities from the bands observed in the case of butene

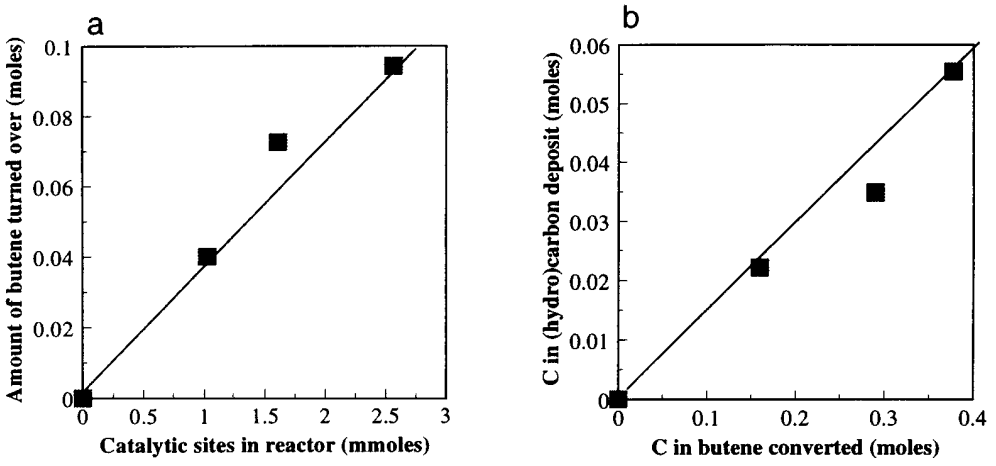


**FIG. 15.** (a) Variation of integral butene turnover with the amount of acid sites in the alkylation system; (b) variation of C in (hydro)carbon deposit on the catalyst with C in converted butene.

oligomerization in Figs. 16c and d. Bands between 3000 and 3200 $cm^{-1}$, generally attributed to aromatic deposits, were not observed. However, a small peak at 1590 $cm^{-1}$, attributed to polyaromatic coke (23) is also seen. The bands observed at 1372, 1487, and 1642 $cm^{-1}$ are commonly attributed to paraffinic oligomers (23).

## DISCUSSION

*The overall reaction mechanism.* Butene participates in two competing reactions, alkylation and oligomerisation. As to be expected from the elementary equations, it has been shown (14, 15) that butene dimerization follows second-order kinetics, while alkylation is first order with respect to n-butene. Thus, low concentrations of n-butene in the reactor are mandatory to suppress oligomerization. It should be emphasized at this point that the true concentration of butene in the liquid phase in the reactor will be significantly lower than the nominal concentration, as butene tends to adsorb strongly on the acid sites. Thus, as long as the catalyst is active, the largest fraction of butene will be adsorbed on the acid sites. This has led to the suggestion of Mesters *et al.* to use the detectability of n-butene in the reactor effluent as indicator of catalyst activity (14). On

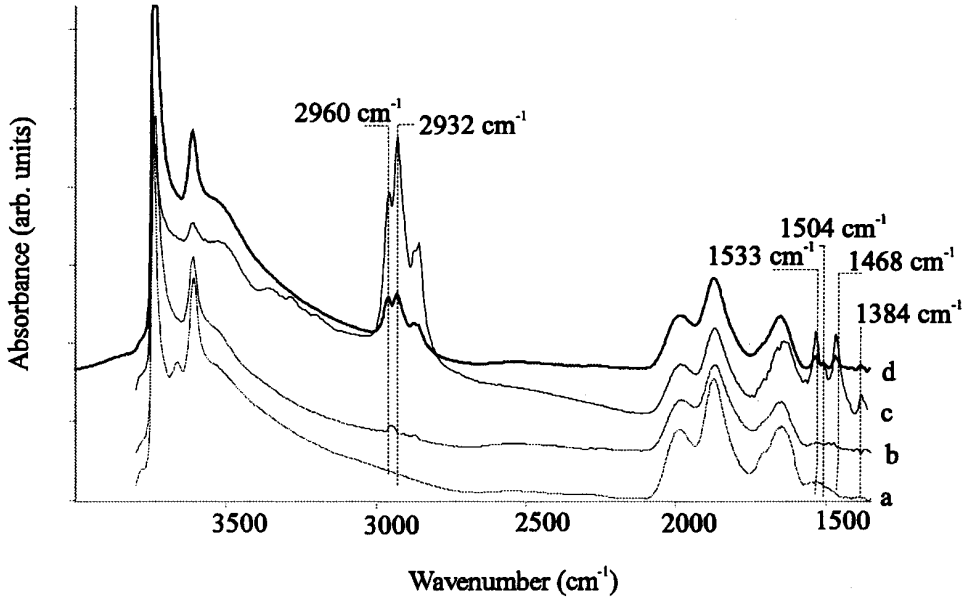


**FIG. 16.** Normalised FT-IR spectra of (a) activated H-BEA; (b) isobutane (1 mbar) on sample (a); (c) butene ($10^{-3}$ mbar) on sample (a); and (d) butene ($10^{-3}$ mbar) on sample (b); all measurements at 348 K.

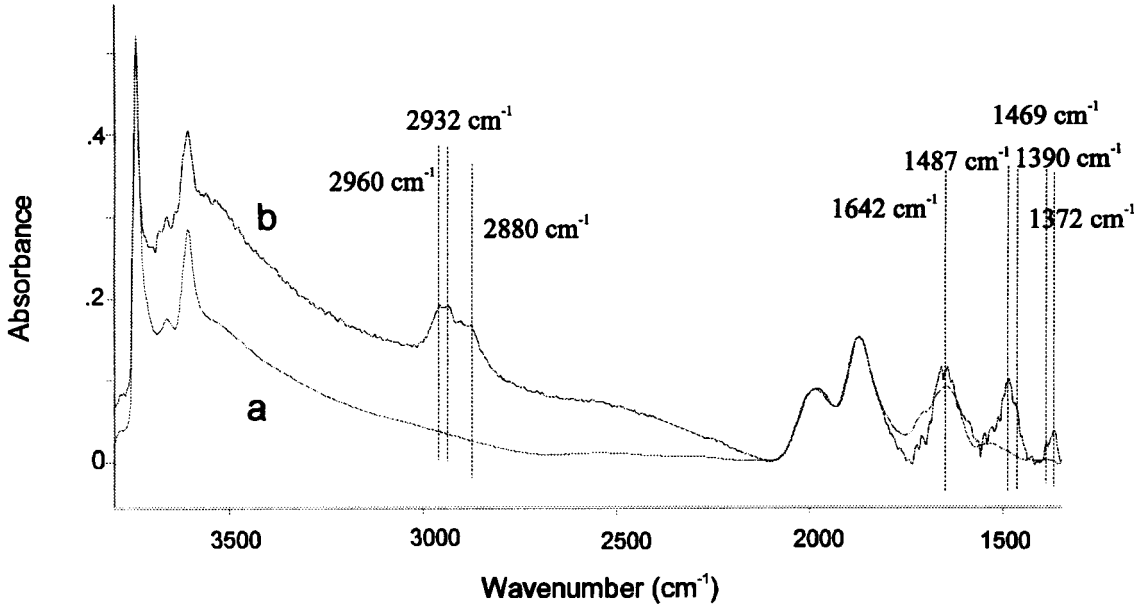


**FIG. 17.** FT-IR spectra of (a) fresh and (b) deactivated BEA at 348 K.

a weight basis of used butene the elementary equations suggest that per converted butene two times the weight of isooctanes must be produced for alkylation, while the weight of products equals that of the reactant for di(oligo)merization. According to both indicators, alkylation was the dominating reaction in all cases and deactivating catalysts could be clearly characterized with these indicators.

Let us first discuss the simplified mechanistic scheme for alkylation presented in Fig. 18. It is seen that alkylation is initialized by the chemisorption of butene forming an butoxy-group that can react with another butene. Because of the low temperature of reaction hydride transfer from iso-butane is required to aid desorption of this species as iso-octane. Intuitively, it is straightforward to accept that higher olefin concentrations would favor further reactions of the alkoxy groups with butenes forming larger alkoxy groups that are more difficult to desorb via hydride transfer.

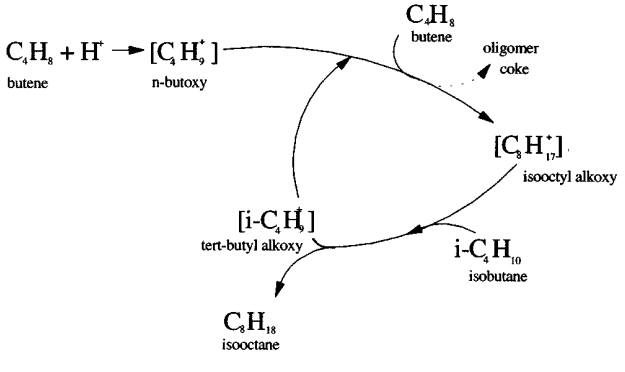


**FIG. 18.** The classical mechanism of isobutane alkylation with butene. The alkoxy species shown schematically are bound to the catalyst surface.

If we transfer this rather abstract situation to the chemistry in the pores of zeolite BEA we need to consider that the zeolite grain will induce a concentration gradient of alkenes in the pores. Knowing that butene is more strongly adsorbed than isobutane we can assume that the butenes are first saturating the zeolite and are certainly faster transported in the pores than isobutane. This leads to a higher reactivity inside a grain which in itself restrains the hydride transfer reaction.

Indeed, initially the trimerization (or double alkylation of an butoxy group) is favored leading to a heavier alkylate (see Fig. 8). The high TMP/DMH ratios observed at short times on-stream (see Fig. 6) indicates that this multiple alkylation is different from butene dimerization observed at later time on-stream in deactivating catalysts leading to DMH formation presumably on weak acid sites. At a certain constant percentage of the total number of Brönsted sites, the alkoxy group will not only be alkylated twice, but three to four times. These species seem to be too large or too bulky to be transported out of the pores under typical reaction conditions. It can be safely assumed that such deactivation would be more pronounced in the core of a crystallite than on the outside. With time on stream, however, the inactive core will increase and eventually only the zeolite outside may be active. In line with model two observations were made; i.e., the contribution of the heavier alkylate decreased (see the quite rapid drop in selectivity after 15 h time on-stream in Fig. 8) and the theoretical yield of twice the weight of the n-butene feed is approached. It is interesting to notice that at longer time on stream, i.e.,

when the catalyst starts deactivating (butene is detected in the liquid phase), the selectivity to heavier products increased again at the expense of iso-octanes. In this phase we would like to speculate that insufficient sites exist on the outer surface of the zeolite particle to sorb or convert all butene molecules leading to a self-enhancement of the deactivation through kinetically favoring multiple alkylation and dimerization on weak acid sites over hydride transfer.

*(Hydro)carbon deposition on the catalyst.* While we have established that multiple alkylation is especially pronounced at initial time on stream and in the phase of catalyst deactivation, we turn to the model experiment to demonstrate the nature of the deposits that cause deactivation. IR spectroscopy indicates the formation of alkoxy species that grow via oligomerization. In a gas phase experiment the degree of that oligomerization is significantly lower in the presence of isobutane than in its absence. The difference between the IR spectrum of the deactivated catalyst and those with oligomeric butene species suggests that the catalyst deactivation is related to the presence of bulky polyalkylate material at the active sites rather than the typical butene oligomer.

In order to estimate the length of these alkoxy deposits we use the overall mass balance of one experiment. In the yield profile curve of Fig. 9, the shaded area (below the 204 wt% yield) corresponds to the hydrocarbon deposited on the catalyst after subtracting the fractions of butene needed for initiation, multiple alkylation, and retarded desorption. Therefore, on an average, about 10 wt%, or 4 of the 40 butene molecules turning over per site, or the equivalent of a hexadecoxy group, deactivates a catalytic site on H-BEA. Thus, to deactivate the acid site the mechanistic cycle depicted in Fig. 18 occurs up to three times on a catalyst site. In each cycle one butene molecule is consumed towards the formation of a larger alkoxy group. As the cycle repeats, the efficiency of desorption by hydride transfer decreases and the large alkanes resulting from multiple alkylation reactions (mostly $C_{12}$ and above) preclude easy transport and further reaction. However, since the selectivity to form this deposit is only 10.5 wt% of the total butene converted, stable catalyst activity is observed for an extended time.

*The role of the reaction temperature.* Figure 5 shows that the optimum temperature for the production of iso-octanes was approximately 350 K. At lower reaction temperatures more of the higher molecular weight alkylate was formed, at higher temperatures cracking to small moleclues became important. The 350 K is significantly higher than the optimum of approximately 308 K reported by Simpson *et al.* (6) for alkylation over USHY in a fixed bed reactor and the 250 K reported by Olah *et al.* (24) for alkylation with trifluoromethanesulfonic acid as catalyst. One explanation for the poorer selectivity to $C_8$ alkanes at lower temperatures is that at lower temperatures hydride transfer (having a higher energy of activation than alkylation of an alkoxy group by butene [25]) is less favored. This corresponds to the observation of lower olefin conversion at lower temperatures in fixed bed conditions by Corma *et al.*, induced by very rapid deactivation of the catalytically active sites (10) and, consequently, also higher selectivities to products of oligomerisation reactions (11). One possible explanation for the lower TMP/DMH ratio at higher temperatures is that at those temperatures (383 K, 423 K), the rate of isomerisation of 2-butene to 1-butene is higher and the higher production rate of 1-butene results in lower TMP selectivities (6). As the temperatures increase above 350 K the higher apparent energies of activation for cracking (25) begins to favor this route over the others.

*Iso-octane selectivity.* After showing that an optimum temperature window for production of iso-octanes exists one needs to address the factors influencing the distribution of the octane isomers. In this regard, two issues are to be raised, i.e., the relation between TMPs and DMHs and the distribution among these two groups of isomers.

The enthalpies of the interaction of TMPs and DMHs with the acid sites of H-BEA are not expected to be significantly different. Further, the diffusivities of TMP and DMH were nearly identical in zeolite H-BEA (26). As TMP is the dominating product, but DMH is thermodynamically favored, we conclude that the $C_8$ skeletal isomer selectivity is kinetically controlled. It also suggests that the isomerization from TMP to DMH is very slow compared to all other reaction rates.

As depicted schematically in Fig. 18 adsorbed octane alkoxy species desorb as alkanes by hydride transfer from isobutane. With zeolite BEA 2,2,4-TMP was found in all studies to be the dominating product. As can be seen in Fig. 10, it is also the thermodynamically most favored TMP isomer. However, because 2,2,4-TMP is rather unlikely to form as the initial product of alkylation, it must be formed via isomerization of a primarily formed alkoxy group. Thus, we speculate that the selectivity within the TMP isomers is driven by thermodynamics and the residence time to isomerize before desorption as alkane. The question arising then is whether it is a one-step process or whether an iso-octane can desorb and then readsorb and be isomerized.

To probe that we have preadsorbed n-octane prior to a standard reaction and did not observe conversion of n-octane under all experimental conditions tested. Thus, we conclude that in a typical alkylation experiment desorbed alkanes do not react further. This is attributed to the fact that effectively competing with the iso-butane (about a 20-fold molar excess) for hydride transfer is hardly possible and that isomerization of alkanes is very slow below 373 K in the absence of reduced metals. This situation is different from observations for strong liquid acids such as sulfuric acid where molecules like the trimethylpentanes (27) are known to undergo further reactions. Additional evidence for the lack of reactivity of the product alkylate

($C_8$ paraffins) over solid acids, once they are desorbed from the surface of the catalyst comes from the data of Mostad *et al.* (28). Alkylation in a semi batch system (with long reaction times) did not indicate variations of the $C_8$ isomer selectivity as a function of time on stream once butene conversion was complete.

As isomerization must, thus, occur in the state of the octane alkoxygroup, the results indicate that sufficient time for isomerization must have existed before hydride transfer occurred. If that is correct the TMP distribution should correspond more to the thermodynamic equilibrium, the slower the hydride transfer is. In conclusion, we would like to stress that a higher hydride transfer rate, realized by whatever means, will shift the product distribution from 2,2,4-TMP to 2,2,3-TMP and 2,3,4-TMP. It should be remembered here that higher concentrations of framework Al (strong Brønsted acid sites) (29) improves hydride transfer rates.

Under most experimental conditions, the $C_8$ isomer selectivity was found to be practically constant until the catalyst deactivated. When operating at very low olefin space velocities (0.02–0.05 $h^{-1}$), also prolonging the catalyst lifetime (see Fig. 13), the selectivity to 2,2,4-TMP increased at the expense of the selectivity to 2,3,4-TMP. Following the above arguments this indicates a gradual decrease of hydride transfer rates.

The last question in this respect has to address the primary selectivity of the alkylation process as compiled in Scheme 1:

*Alkylation with 2-butene*,

$$CH_3{-}CH(CH_3){-}CH_3 + CH_3{-}CH{=}CH{-}CH_3 \rightarrow CH_3{-}C(CH_3)_2{-}CH(CH_3){-}CH_2{-}CH_3 \quad \text{(2,2,3-TMP)} \qquad [1]$$

*Alkylation with 1-butene*,

$$CH_3{-}CH(CH_3){-}CH_3 + CH_2{=}CH{-}CH_2{-}CH_3 \rightarrow CH_3{-}C(CH_3)_2{-}CH_2{-}CH_2{-}CH_2{-}CH_3 \quad \text{(2,2-DMH)} \qquad [2]$$

*Alkylation with isobutene*,

$$CH_3{-}CH(CH_3){-}CH_3 + C(CH_3)_2{=}CH_2 \rightarrow CH_3{-}C(CH_3)_2{-}CH_2{-}C(CH_3){-}CH_3 \quad \text{(2,2,4-TMP).} \qquad [3]$$

Scheme 1 indicates that DMH is formed as primary product from alkylation with 1-butene. Indeed, Nowak *et al.* (30) and Simpson *et al.* (6) speculated that the DMHs may appear as important product of alkylation of isobutane with 1-butene. Our experiments indicate that the choice of butenes does not alter the $C_8$ isomer selectivity. It is likely that a thermodynamic distribution of linear $C_4$ alkenes exists under alkylation conditions on BEA zeolite. This observation is a marked difference from the report of Collins *et al.* (21) who found that the product of isobutane alkylation on $BF_3/SiO_2$, a Lewis acid catalyst was sensitive to the choice of 1-butene or 2-butene for the reaction. Collins *et al.* (21) speculated that the lower degree of linear butene isomerisation observed with $BF_3/SiO_2$ is due to the complex formation between $BF_3$ and the olefin preserving 1-butene for direct alkylation and, consequently, producing more DMH. If transferable, this suggests also that while isomerization of TMPs (involving methyl shifts) is possible, isomerization involving a branching reaction (the DMH to TMP reaction) seems hardly possible. The observed isomer selectivity indicates the practical absence of 2,2-DMH, the isomer expected from the reaction between isobutane and 1-butene (see Scheme 1). It should also be noted that although isobutene is thermodynamically the most favored butene isomer at 350 K, the skeletal isomerisation of butene is energetically a more demanding reaction and seems not to occur over acidic zeolites to any substantial extent at these temperatures. The data of Butler and Nicolaides (31) which report that iso-butene is not formed from 1-butene at temperatures below 573 K on H-ZSM-5 supports this view.

*Influence of Lewis acid sites.* Corma *et al.* (13) suggest that while some of these extraframework species acting as Lewis acid sites are detrimental to catalytic activity, others combine synergistically with Brønsted sites to produce Brønsted acid sites of enhanced acidity. The BEA catalyst of this study has a finite concentration of Lewis sites as can be seen from pyridine sorption experiments. It is also known that Lewis sites interact more strongly with unsaturated hydrocarbons such as butene than Brønsted sites. As in the absence of protons, the reaction of olefins under the present reaction conditions is limited to double bond isomerization, the primary effect of the Lewis acid sites seems to be to enhance the concentration of butene close to the catalytically active Brönsted acid sites. Indirect influences of the Lewis acid sites on the strength of the Brönsted acid sites cannot be assessed at present and will be subject to further investigation.

## CONCLUSIONS

Alkylation over zeolite catalysts seem to be a subtle balance of alkylation, hydride transfer, and cracking reactions. Due to the complex interplay of several elementary reactions the reactivity and selectivity is very sensitive to small variations in the reaction conditions and the properties of the catalytic materials. H-BEA is in that respect a relatively robust catalysts and has therefore been chosen to mechanistically discuss the alkylation of iso-butane with n-butene.

Alkylation on the H-BEA catalyst has an optimal temperature of 350 K, while pressures between 20–50 bar do

not significantly influence catalyst activity, lifetime, or alkylate selectivity. At temperatures higher than 350 K cracking dominates; at lower temperatures multiple alkylation dominates. Under these optimal reaction conditions catalyst lifetimes of 15 h could be achieved using an olefin space velocity of 0.2 $h^{-1}$. Three distinct regimes of catalyst action were identified as a function of time on stream, i.e., an initial regime of multiple alkylation leading to high initial selectivities to $C_{9-12}$ compounds, a regime of stable alkylation producing essentially $C_8$ alkanes and, finally, a catalyst deactivation regime during which olefins are formed. Prior to the activity decay, the product stream is exclusively paraffinic, indicating that zeolite H-BEA effectively catalyzes hydride transfer.

During the period of stable operation product yields close to 204 wt% (on the basis of butene fed to the reactor) indicate that alkylation is the principal reaction occuring. Oligomerization only occurs during the deactivation period. IR spectroscopy of the deposits on H-BEA after reaction shows that the species blocking active sites are highly branched alkoxy species resulting from (multiple) alkylation reactions and not products of butene oligomerization. Brønsted acid sites retain their activity for a fixed turnover number of 40, during which the low selectivity to polyalkylate causes deposits to build up slowly, leading ultimately to a blockage of these sites by $C_{16}$-type species.

With respect to the composition of the alkylate it is seen that among the $C_8$ paraffins TMPs dominate and the thermodynamically more favored DMHs are observed to a much lesser extent. This is directly the consequence of the dominating alkylation with 2-butene and the fact that while the methyl shift within the $C_8$ alkoxy groups seems facile, skeletal isomerisation hardly seem to occur. In contrast within a group of $C_8$ isomers, isomerization is much more rapid and the isomer distribution seems to be determined by the rate of isomerization in the adsorbed state and hydride transfer from iso-butane.

## ACKNOWLEDGMENTS

The funding for this work by the European Commission (EC Contract JOF3-CT95-0023) under the auspices of the Joule Thermie program is gratefully acknowledged.

## REFERENCES

1. Rao, P., and Vatcha, S. R., *Preprints* **41**(4), 685 (1996).
2. Albright, L. F., and Li, K. W., *Ind. Eng. Chem. Process Des. Develop.* **9**(3), 447 (1970).
3. Lindahl, C. B., and Mahmood, T., *in* "Encyclopedia of Chem. Tech." (M. Kroschwitz, Exec. Ed.), Vol. 11, 4th ed., p. 267. Wiley, New York, 1994.
4. Corma, A., and Martinez, A., *Catal. Rev. Sci. Eng.* **35**(4), 483 (1993).
5. Van Brugge, P. T. M., De Groot, C., Mesters, C. M. A. M., and Pfeferoen, D. G. R., European Patent Appl. 0640 575 A1, 1994.
6. Simpson, M. F., Wei, J., and Sundaresan, S., *Ind. Eng. Chem. Res.* **35**, 3861 (1996).
7. Huss, A., Jr., Kirker, G. W., Keville, K. M., and Thomson, R. T., U.S. Patent 4,992,615, 1991.
8. Husain, A., World Patent Appl. WO 94/0315, 1994.
9. Husain, A., Huss, A., Jr., and Rahmim, I. I., U.S. Patent 5,475,175, 1995.
10. Corma, A., Gómez, V., and Martinez, A., *Appl. Catal. A* **119**, 83 (1994).
11. Corma, A., Juan Rajadell, M. I., Lopez-Nieto, J. M., Martinez, A., and Martinez, C., *Appl. Catal. A* **111**, 175 (1994).
12. Fan, L., Nakamura, I., Ishida, S., and Fujimoto, K., *Ind. Eng. Chem. Res.* **36**, 1458 (1997).
13. Corma, A., Martinez, A., Arroyo, P. A., Monteiro, J. L. F., and Sousa-Aguiar, E. F., *Appl. Catal. A* **142**, 139 (1996).
14. Mesters, C. M. A. M., Pfeferoen, D. G. R., Gilson, C., van Brugge, P. T. M., and de Jong, K. P., *Appl. Catal. A*, submited.
15. De Jong, K. P., Meesters, C. M. A. M., Pfeferoen, D. G. R., van Brugge, P. T. M., and De Groot, C., *Chem. Eng. Sci.* **51**(10), 2053 (1996).
16. Eder F., and Lercher, J. A., *J. Phys. Chem. B* **101**, 1273 (1997).
17. Zhan, Z., Ph.D. thesis, University of Twente, 1995.
18. Stockenhuber, M., and Lercher, J. A., *Microp. Mater.* **3**, 457 (1995).
19. Klinowski, J., *Anal. Chim. Acta.* **283**, 929 (1993).
20. Borade, R., and Clearfield, A., *J. Phys. Chem.* **96**, 6729 (1992).
21. Collins, N. A., Child, J. E., and Huss, A., *Preprints Am. Chem. Soc.* **41**(4), 706 (1996).
22. Becker, L., and Förster, H., *Appl. Catal. A* **153**(1–2), 31 (1997).
23. Flego, C., Kiricsi, I., Parker, W. O., Jr., and Clerici, M. G., *Appl. Catal. A* **124**, 107 (1995).
24. Olah, G. A., Surya Prakash, G. K., Török, B., and Török, M., *Catal. Lett.* **40**, 137, (1996).
25. Guisnet, M., and Gnep, N. S., *Appl. Catal. A* **146**, 33 (1996).
26. Nivarthy, G. S., Seshan, K., and Lercher, J. A., unpublished work.
27. Ende, D. J., and Albright, L. F., *Ind. Eng. Chem. Res.* **33**, 840, (1994).
28. Mostad, H., Stocker, M., Karlsson, A., Junggreen, H., and Hustad, B., *in* "Proc. 11th Int. Zeolite Conf., Seoul, 1996," in press.
29. Mota, C. J. A., Esteves, P. M., and De Amorim, M. B., *J. Phys. Chem.* **100**, 12418 (1996).
30. Nowak, A. K., Mesters, C. M. A. M., Rigby, A. M., and Schulze, D., *Preprints, Am. Chem. Soc.* **41**(4), 668 (1996).
31. Butler, A. C., and Nicolaides, C. P., *Catal. Today* **18**, 443 (1993).